Absorption and Flux Density Measurements in an Iron Plug in R1

AE-13

Ragnar Nilsson and Josef Braun

AKTIEBOLAGET ATOMENERGI

STOCKHOLM · SWEDEN · 1958

Absorption and Flux Density Measurements in an Iron Plug in R1

Ragnar Nilsson and Josef Braun

Summary:-

Thermal, epithermal and fast neutron fluxes have been measured in a 60 cm long, "sliced" iron plug, which has been placed in the lower iron lid of the Swedish reactor R 1. Au foils, Cu foils, Mn foils, P packets, Cu wires and small Fe cylinders have been used. The gamma flux has been determined with film dosimeters.

The measurements have shown that only in the first centimeters of the iron is the activation determined by the thermal flux, which decreases with a relaxation length $\lambda = (1.51 \pm 0.02)$ cm. The epithermal flux is entirely predominant already after 10 cm ($\lambda = 16$ cm). The epithermal neutron flux decreases even more slowly than the fast flux ($\lambda = 6.2$ cm).

Completion of manuscript August 1958
Printed November 1958

LIST OF CONTENTS

Absorption and Flux Density Measurements in an Iron Plug in R 1.

1. Measurement of thermal and epithermal neutron flux

Theory

Thermal and epithermal fluxes are usually determined by irradiating rather thick (10 - 100 mg/cm^2) metal foils with respectively without cadmium. Subsequently the foil activity from (n, γ)-reactions is measured.

Let n(x) and $n_{Cd}(x)$ define the counting rates when measured on a bare foil of thickness x, and respectively on a foil covered with cadmium of thickness y. Both counting rates are corrected to saturation and to the end of the irradiation time. The counting rates can be divided into thermal and epithermal components, $n_t(x)$, respectively $n_{epi}(x)$. For calculating purposes, Martin [1] has suggested the introduction of the following three parameters: the cadmium ratio $R_{Cd}(x)$, and the correction factors F and X. F takes into consideration the absorption of the epithermal neutrons, and X the leakage of the thermal neutrons through the cadmium cover. The relation between these quantities appears from the following diagram, where

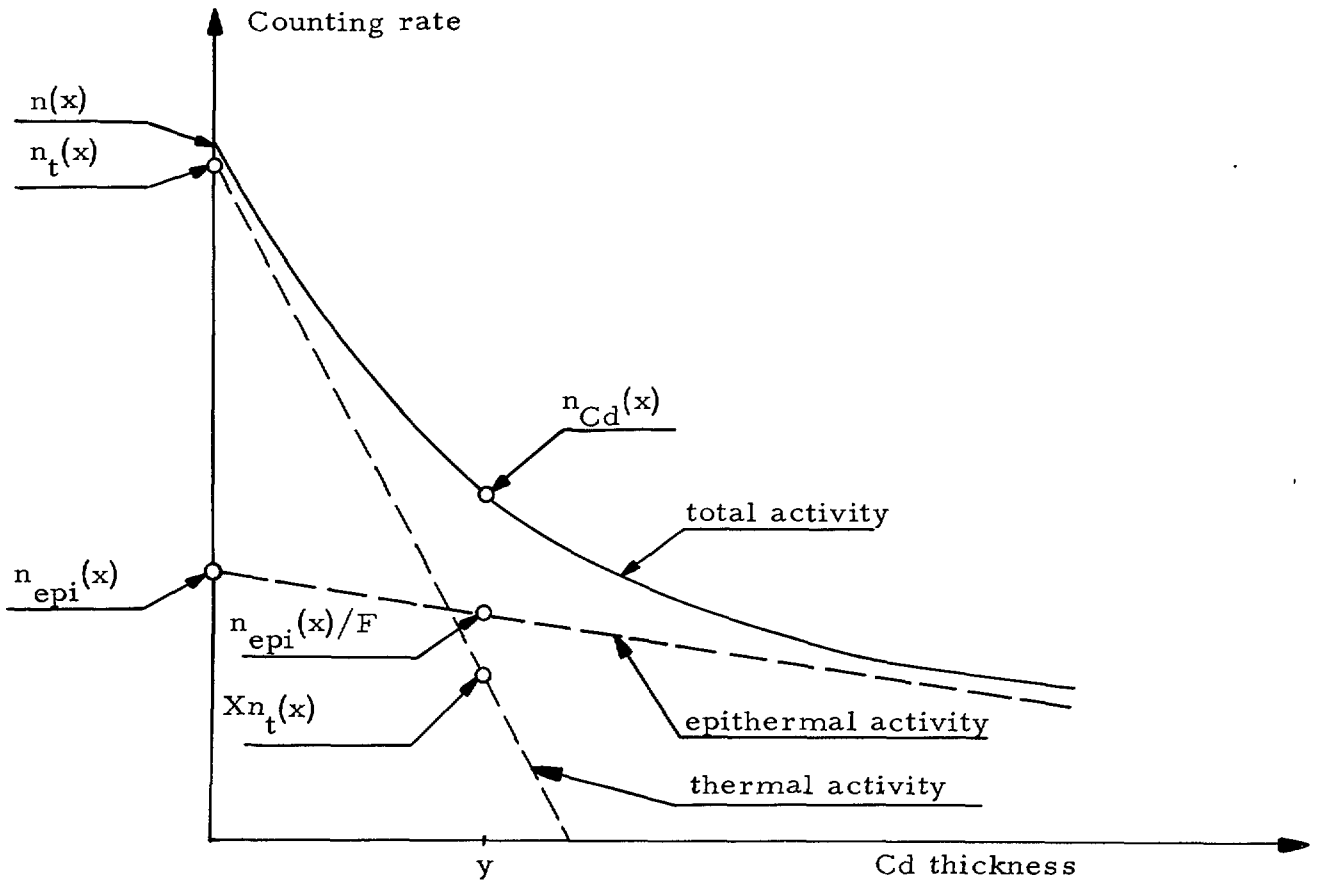

Activity from a foil of thickness x versus the thickness of the cadmium cover.

the activation has been plotted in a logarithmic scale as a function of a supposed varying cadmium thickness, and from the following equations.

$$R_{Cd}(x) = \frac{n(x)}{n_{Cd}(x)} \tag{1}$$

$$n_t(x) = \frac{n(x) - F\, n_{Cd}(x)}{1 - XF} \tag{2}$$

$$n_{epi}(x) = F\left[n_{Cd}(x) - X\, n_t(x) \right] \tag{3}$$

As a good approximation, one can often write F = 1 and X = 0.

In the measurements one looks for the ratio Q between the activation of the thermal and epithermal neutrons. With the usual notations one obtains

$$Q = \frac{\phi_t \sigma_{th}}{\int_{E_{min}}^{\infty} \frac{q}{\xi N \sigma_s} \sigma_a(E) \frac{dE}{E}} . \tag{4}$$

Greenfield et al.[2] have pointed out, that the relation between $n_t(x)$ and $n_{epi}(x)$ is not the same as the desired ratio Q. The thermal activation is induced rather homogeneously in the foil, since thermal neutrons are only moderately absorbed. The epithermal neutrons, however, are often absorbed in the surface of the foil, due to a corresponding very high resonance cross section. The self-absorption in the foil will therefore be different in the two cases.

Greenfield has also demonstrated a method for calculating the effect of the above mentioned phenomena and employed it for indium foils. The method is based upon the fact that this correction disappears for infinitely thin foils. Greenfield defines two auxiliary functions $G_t(x)$ and $G_{epi}(x)$ by the following equations

$$n_t(x) = G_t(x)\, n_t(o), \qquad n_{epi}(x) = G_{epi}(x)\, n_{epi}(o) \tag{5}$$

These functions depend only on the properties of the detector, of the foil, and of the cadmium. It is essential that the above

functions are independent, however, of the location of the irradiation in the reactor. The following formulas are obtained by introducing the macroscopic, thermal activation cross section Σ, the activation I (with similar subscripts as the counting rate n) and two calibration constants ω and $\omega_t(x)$ characteristic for the counter

$$I_t(o) = \frac{n_t(o)}{\omega} = \frac{n_t(x)}{\omega G_t(x)} = \frac{n_t(x)}{\omega_t(x)} \tag{6}$$

$$I_{epi}(o) = \frac{n_{epi}(o)}{\omega} = \frac{n_{epi}(x)}{\omega G_{epi}(x)} = \frac{n_{epi}(x)}{\omega_t(x) \cdot G_{epi}(x)/G_t(x)} \tag{7}$$

Combining the equations (1) - (7), the result is

$$\phi_t \Sigma = I_t(o) = \frac{1}{\omega_t(x)} \frac{n(x) - Fn_{Cd}(x)}{1 - XF} \tag{8}$$

$$I_{epi}(o) = \frac{1}{\omega_t(x)} \cdot \frac{G_t(x)}{G_{epi}(x)} \frac{Fn_{Cd}(x)\left[1 - XR_{Cd}\right]}{1 - XF} \tag{9}$$

$$Q = I_t(o)/I_{epi}(o) \tag{10}$$

Experimental determination of $\Sigma\omega_t$, ω_t, F, X and G_{epi}/G_t.

Two sets of GM-tubes (halogen quenched end window tubes, Mullard MX 123) were calibrated by irradiating Au, Cu and Mn foils (10 x 10 mm^2) in the central channel at the center of R1. The absolute saturation activity $I_t(o)$ of the Au foils was determined by a β-γ-coincidence method[3]. Thus ω_t for the Au foils was obtained with a standard deviation of $\pm$ 1.5 %, and consequently ϕ_t($\pm$ 2 %) could be calculated by Eq. (8). The known flux was then used for computing $\Sigma\omega_t$ and ω_t for the Cu and Mn foils. The accuracy of these determinations was $\pm$ 2 % respectively $\pm$ 10 % for the Cu foils, and $\pm$ 2.5 %, respectively $\pm$ 3.5 % for the Mn foils. In these calculations, the following value of the activation cross sections have been used:

Σ_{Au} = 0.302 cm^2/g, Σ_{Cu} = 0.0256 cm^2/g, and Σ_{Mn} = 0.147 cm^2/g.

F could be determined by irradiating foils covered with cadmium of different thicknesses (0.13 - 2 mm). The following result was obtained:

Au(18.3 mg/cm^2):F = 1.008 ± 0.002 with 0.5 mm Cd

Cu(73.4 mg/cm^2) : F = 1.028 ± 0.005 - " -

Mn(125 mg/cm^2) : F = 1.029 ± 0.006 - " -

It can be mentioned as a comparison that Martin found a value of 1.02 for Au foils with 1 mm of cadmium. F is of particularly importance, when determining the thermal flux at points, where R_{Cd} is close to 1.

Also X could be determined form the measurements with the Cu and Mn foils. The result was X = 0.0023 ± 0.0004. Evidently this correction is of importance only for measurements of epithermal activity at points where the cadmium ratio is large (cf. Eqs. 8 and 9). Martin gives a value of X = 0.002 for a cadmium thickness of 0.5 mm.

Au foils of different thickness (0.16 - 73 mg/cm^2) were also irradiated with and without cadmium in order to determine G_{epi}/G_t for the GM tube geometry and for the used thickness of Au and Cd. In order to determine the corresponding G_{epi}/G_t for the Mn foils, we also irradiated "infinitely thin" Mn foils (0.04 mg/cm^2) with and without cadmium. The result was:

G_{epi}/G_t = 0.61 ± 0.03 for Au (18.3 mg/cm^2)

G_{epi}/G_t = 0.72 ± 0.02 for Mn (125 mg/cm^2) x)

2. Measurement of the fast neutron flux

For the fast flux the reaction P^{31} (n, p)Si^{31} was used(4). Various investigators have reported different values of the

x) Lately G_{epi}/G_t has also been preliminary determined for Cu, with evaporated foils (0.015 mg/cm^2). G_{epi}/G_t = 0.83 ± 0.15. This factor has not been used in the plotted Cu activities.

half-life of Si^{31}, for instance Hughes[5] 170 m, Lüscher[6] 155 m. A determination of the half-life was therefore made, which gave (155 ± 3) m.

In order to calibrate the GM tube arrangements Si packages with the same weight and shape as the P packages were activated in a known thermal flux. The packages consisted of rings of plexiglass (outer diam. 24 mm, inner diam. 18.5 mm, height 1 mm) with 20 μ:s Al foils glued on. They had been filled with about 420 mg phosphorus, respectively silicon. In the measurements, corrections were made for the difference in self-absorption (<5 %) between foils of somewhat different thickness. Besides the desired Si^{31} activity we also obtained P^{32} activity (14.3 d) and an activity with a half-life of about 15 hours. The latter probably arose from impurities in the phosphorus. The influence of both activities was eliminated by plotting decay curves for the different samples.

In the calculation of the total fast flux, the value (110 ± 10) mb has been used as the activation cross section for Si^{30} (n, γ) Si^{31}. Hughes reports a value of 19 mb as the average cross section for the P^{31} (n, p) Si^{31} reaction over the whole unmoderated fission spectrum. He estimates the error in this cross section to a factor 2.

Ricamo[7] has measured the cross section for the (n, p) reaction in the energy interval 1.9 - 3.6 MeV. By means of these values, the average cross section over the whole fission spectrum has been graphically calculated to (25 ± 3) mb, which value has been used in the calculation of the flux. 2.5 MeV was obtained for the effective energy threshold.

3. Measurement of the gamma flux

Film dosimeters (Dupont 508, Dupont 1290) were used in order to determine the gamma flux. The films were wrapped in 0.5 mm lead during the measurements and during the calibration against a Co sample.

4. The iron plug

The measurements were made in a 60 cm long, cylindrical and "sliced" iron plug, which was placed in the lower iron lid of the reactor (Fig. 1). Detectors were placed in cuttings (Ø 25 mm) in the slabs. Fig. 2 demonstrates the construction of the plug and the location of the points of measurement. The measurements were made with and without the 1 mm thick cadmium disk, which could be placed inside a 2 mm thick aluminium disk in the bottom of the plug. There were two vertical holes of 3 mm diameter in the lowest lying iron slab which was 50 mm thick. The activation was measured there with 10 iron cylinders (Ø 3 mm, height 5 mm) and with a copper wire (Ø 1.5 mm), which was afterwards cut into pieces of 5 mm length.

5. Result of the measurements

Errors

The directly measured activities of the foils have in general been determined with a standard deviation below 1 %, and the weights of the foils with an accuracy of 0.4 %. Random errors are therefore mainly of secondary importance, except for the calculation of the thermal flux (proportional against the difference between two measured values, often of almost equal size). The standard deviation is indicated in the diagrams. A comparison between the measured points of the epithermal flux in Fig. 7 or 8 gives a measure of the reproducibility of the values.

The calibration of the foils was made at 0.4 kW, while the actual experiments were performed at power levels between 0.5 and 300 kW. Linearity has been assumed between the flux and the power level, and all the activities have been corrected to the nominal power 300 kW of the reactor. The gamma dose curve, however, (Fig. 12) has not been corrected, but plotted at 1 kW, which is the power level employed during the experiment.

Variation of D_2O-level

The Au and Cu activities were measured at 2 different water levels: 4625.5 and 4568.1 mm, i.e. 67 and 9 mm above the uranium rods (Figs. 3, 4, 5). This decrease in the level of 58 mm increased the epithermal activity with 47 % for the Au foils and with 49 % for the Cu foils at points 400 mm inside the iron. The increase in the total activity is considerably smaller in the bottom of the plug, which is probably due to the decrease of the thermal flux. The decrease of the difference between the points outside and inside the Cd disk seems to confirm this assumption.

Lower part of the iron plug

The activity in the first 50 mm of the iron plug was measured with Cu wire and Fe cylinders (Figs. 5 and 6), both with and without the Cd disk. In order to analyze the curves in Fig. 6, the following assumptions have been made:

1. The activity (155 m, probably from Mn^{56}) is composed of three components:

   a) n_{t1}, due to thermal neutrons which have penetrated into the iron,

   b) n_{t2}, due to epithermal or fast neutrons from the outside, which have been slowed down to thermal neutrons in the iron,

   c) n_{epi}, due to epithermal neutrons in the iron.

2. When the lower part of the iron plug is cover by the Cd disk, $n_{t1} = n_{t2} = 0$ immediately behind the disk.

3. n_{epi} decreases as a pure exponential in the iron with a relaxation length of $\lambda = 7.3$ cm, obtained from Fig. 7.

From Fig. 6 can be concluded that the thermal neutrons coming from the outside are absorbed with a relaxation length $\lambda = (1.43 \pm 0.10)$ cm. It also appears from this figure that by taking away the Cd disk, the activity of the measuring cylinders in the

bottom of the plug increases by a factor 8.7, which after 50 mm iron has already decreased to 1.5. It should be pointed out, however, that these factors are not "G_{epi}/G_t-corrected". It is hardly necessary to point out, that the curve n_{t2} is drawn with a great unaccuracy (a factor of 1.5 - 2).

The somewhat vague depression of n_{t1} in the bottom of the iron plug is possibly due to the influence on the flux of the Cd sheet under the iron lid.

Thermal and epithermal activity in the iron plug

Without Cd disk, the activity is measured with Au, Cu and Mn foils at 9 points in the iron plug (Figs. 7, 8 and 9). In addition, the activity with Cd disk is measured by means of Au and Cu foils. The Cu measurements probably give the most valuable information. They are indeed not "G_{epi}/G_t-corrected", but since this factor probably is close to 1, the activity of iron and its alloying elements can be estimated by means of these curves. In general these elements, like Cu, lack high activation resonances in the epithermal region. The diagrams show that the epithermal activity first decreases with $\lambda = 7.3$ cm, and after 400 mm with $\lambda = 16$ cm. The faster decrease after 500 mm probably depends on the influence of the borated paraffin lid.

As expected, no difference can be shown in the epithermal activity with and without Cd disk, except perhaps in the vicinity of this disk. However, the values at this point with Cd disk in position are somewhat inaccurate. This is because the measurements were made only with bare foils, and because the calculations were based upon the assumption, that the thermal flux is zero behind the disk. The thermal flux can be determined with certainty only by measurements without Cd disk and then only in the bottom of the plug. At the other points the thermal activity contributes with only a few percent to the total activity. Nevertheless the thermal flux has still been calculated at other points, and the values found are shown

with their standard deviations in the diagrams. As previously described, the thermal activity has been divided into two components, of which I_{t1} is assumed to decrease exponentially, while I_{t2} is assumed to follow the shape of the corresponding curve in Fig. 6 in the interval 0-50 mm and thereafter to decrease at the same rate as the epithermal Au activity. The experimental values obtained do not seem to contradict this assumption.

The thermal flux from outside decreases according to the measurements with a relaxation length

$$\lambda = (1.33 \pm 0.20) \text{ cm} \quad \text{(Au)}$$
$$\lambda = (1.52 \pm 0.03) \text{ cm} \quad \text{(Cu)}$$
$$\lambda = (1.54 \pm 0.04) \text{ cm} \quad \text{(Mn)}$$

According to the same measurements the ratio between, the maximum thermal flux with and without Cd disk is correspondingly 70, 190 and 130. It should be observed as a comparison that Fig. 6 gave the values $\lambda = (1.43 \pm 0.10)$ cm and the ratio 100.

The thermal flux in the diagrams refer to the conventional flux.

Starting from I_{epi} in Fig. 7, the slowing down density can be calculated for neutrons with an energy of 4.9 eV. According to a method described by Dayton and Pettus[8] we have calculated an effective "Cd-cut-off", E_{Cd}, related to E_{min} in Eq. (4) by

$$\int_{E_{min}}^{\infty} \frac{q}{\xi N \sigma_s} \sigma_a(E) \frac{dE}{E} = F \int_{E_{Cd}}^{\infty} \frac{q}{\xi N \sigma_s} \sigma_a(E) \frac{dE}{E} . \qquad (11)$$

E_{Cd} for Au, Cu and Mn foils was found to be (0.45 ± 0.01) eV provided the flux is isotropic.

Diametrical Cu ribbon at the bottom of the iron plug

When the activation was made without the Cd disk some influence could be anticipated from the Cd sheet placed under the iron lid. In order to examine this deviation from infinite geometry, a diametrical ribbon was activated at the bottom of the plug (Fig. 10). By means of other measurements with the Cd disk, the activity directly outside and inside this disk could be calculated. A relative activity of 0.710 respectively 0.109 was found. If these values are assumed independent of the radial distance from the center of the plug, and if the activation of the foils inside the Cd disk is assumed to depend completely on epithermal neutrons, the variation of the thermal activation as a function of distance from the center can also be calculated. The surrounding Cd sheet probably also lowers the flux in the center of the bottom of the plug, since no horizontal plateau can be found in the activation curve. The decrease of the thermal activity by the cadmium is therefore possibly somewhat larger than the ratios mentioned in the former paragraph.

The measurements prove further that even if the Cd sheet has influence on the flux, it varies, however, less than 6 % at different distance from the center in the same plane in the iron plug.

Fast flux in the iron plug

According to Fig. 11, the fast flux seems to fall almost exponentially over at least 400 mm. The slope was measured to λ = 6.2 mm. It should be observed that the fast neutrons, at least those over 2.5 MeV, obviously seem to slow down rather rapidly to epithermal neutrons, which then in their turn proceed more easily through the iron plug (λ = 16 cm). It should be noted that the absolute value of the flux is measured provided that the fast neutrons are distributed according to the fission spectrum. This is probably not the case in the iron plug.

Gamma flux in the iron plug

The variation of the gamma flux in the iron plug is shown in Fig. 12. The first, rather fast decrease, λ =3.8 cm, is probably a result of fission gammas. Capture gamma and build-up in the iron apparently change the slope to λ= 13 cm.

It is possible that a part of the film blackening may come from the neutron induced beta radiation in the lead envelope. However, the cross-section for this reaction is rather small.

6. Acknowledgements

The authers are indebted to Dipl.ing. M. Roos for many valuable discussions, and to Ing. E. Brunberg, who has been of great help in carrying out the experimental work.

7. Bibliography

1) D.H. Martin, Nucleonics 13, No. 3, 52 (1955)

2) M.A. Greenfield et al. NAA-SR-1137, Part I (1955)

3) E. Johansson, AEFI-38 (1956), AB Atomenergi, Stockholm

4) E. Johansson, AEFI-71 (1957), AB Atomenergi, Stockholm

5) D.J. Hughes, "Pile Neutron Research", Addison-Wesley, Cambridge (1953)

6) E. Lüscher et al, Helv. Phys. Acta 23, 561 (1950)

7) R. Ricamo, Nuovo Cim. 8, 383 (1951) or
D.J. Hughes and J.A. Harvey, BNL 325, 105 (1955)

8) I.E. Dayton and W.G. Pettus, Nucleonics 15, No. 12, 86 (1957)

8. Figure captions

1) Reactor tank of R 1

2) Iron plug for activation measurements in central channel of R 1

3) Au activity in iron plug at two different water-levels

4) Cu activity in iron plug at two different water-levels

5) Cu activity in lower part of iron plug at two different water-levels

6) "Fe activity" in lower part of iron plug

7) Au activity in iron plug

8) Cu activity in iron plug

9) Mn activity in iron plug

10) Activity of Cu ribbon at bottom of iron plug

11) Fast flux in iron plug

12) Gamma dose rate in iron plug

Reactor Tank of R1

Fig. 1

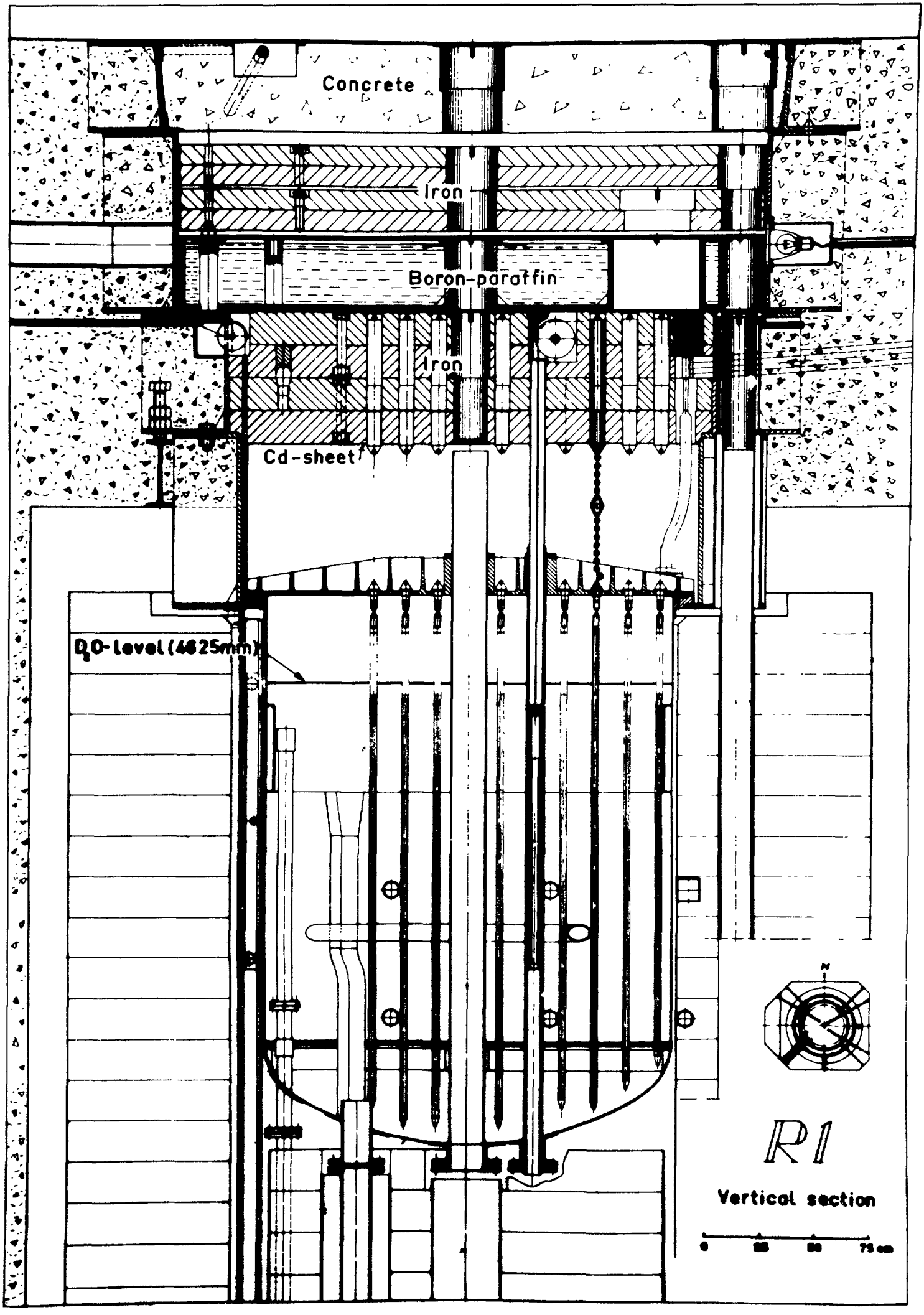

Iron Plug for Activation Measurements in Central Channel of R1

Fig. 2

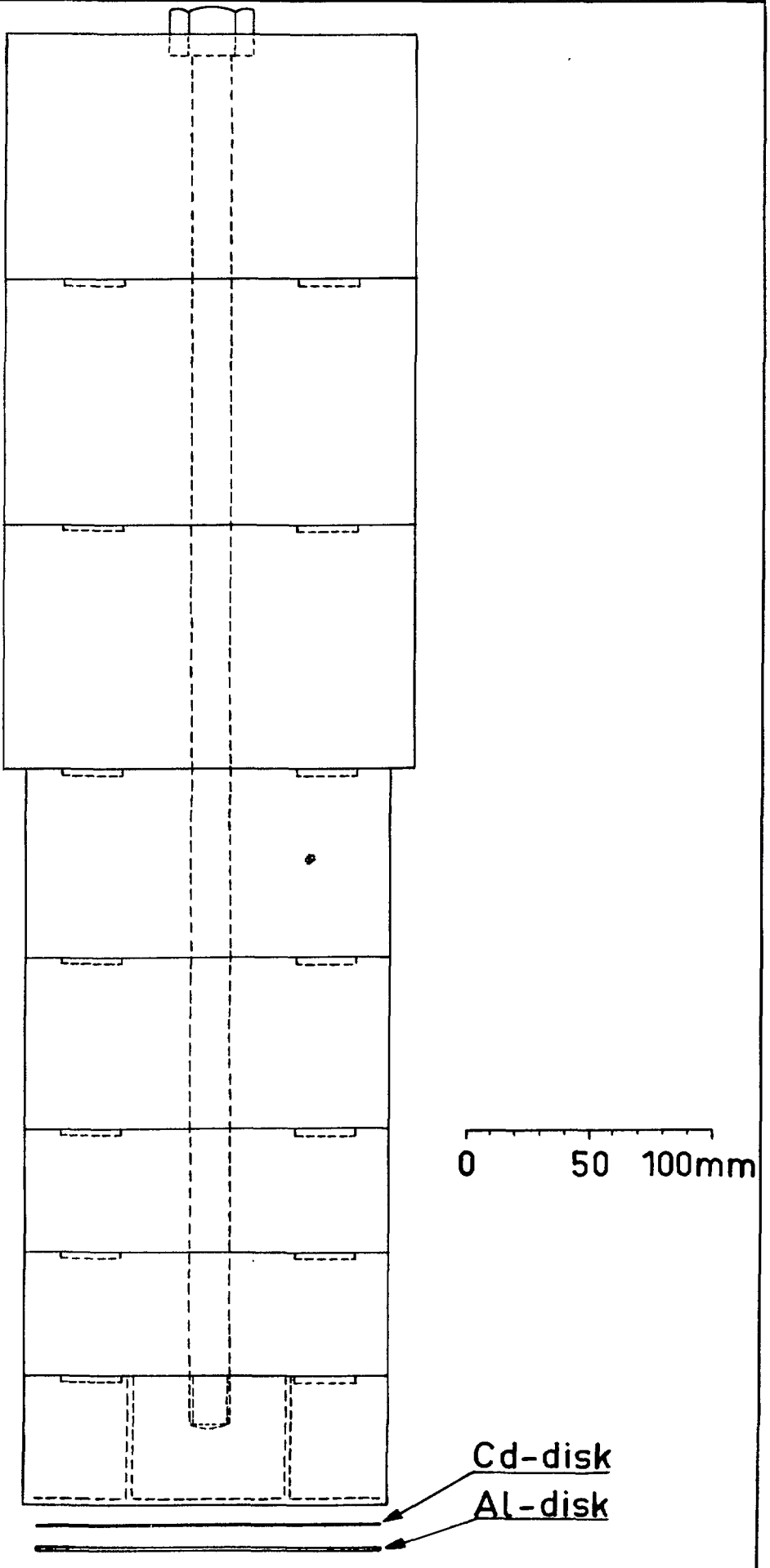

Au-activity in Iron Plug
at Two Different Water-levels
(with Cd-disk)

Fig. 3

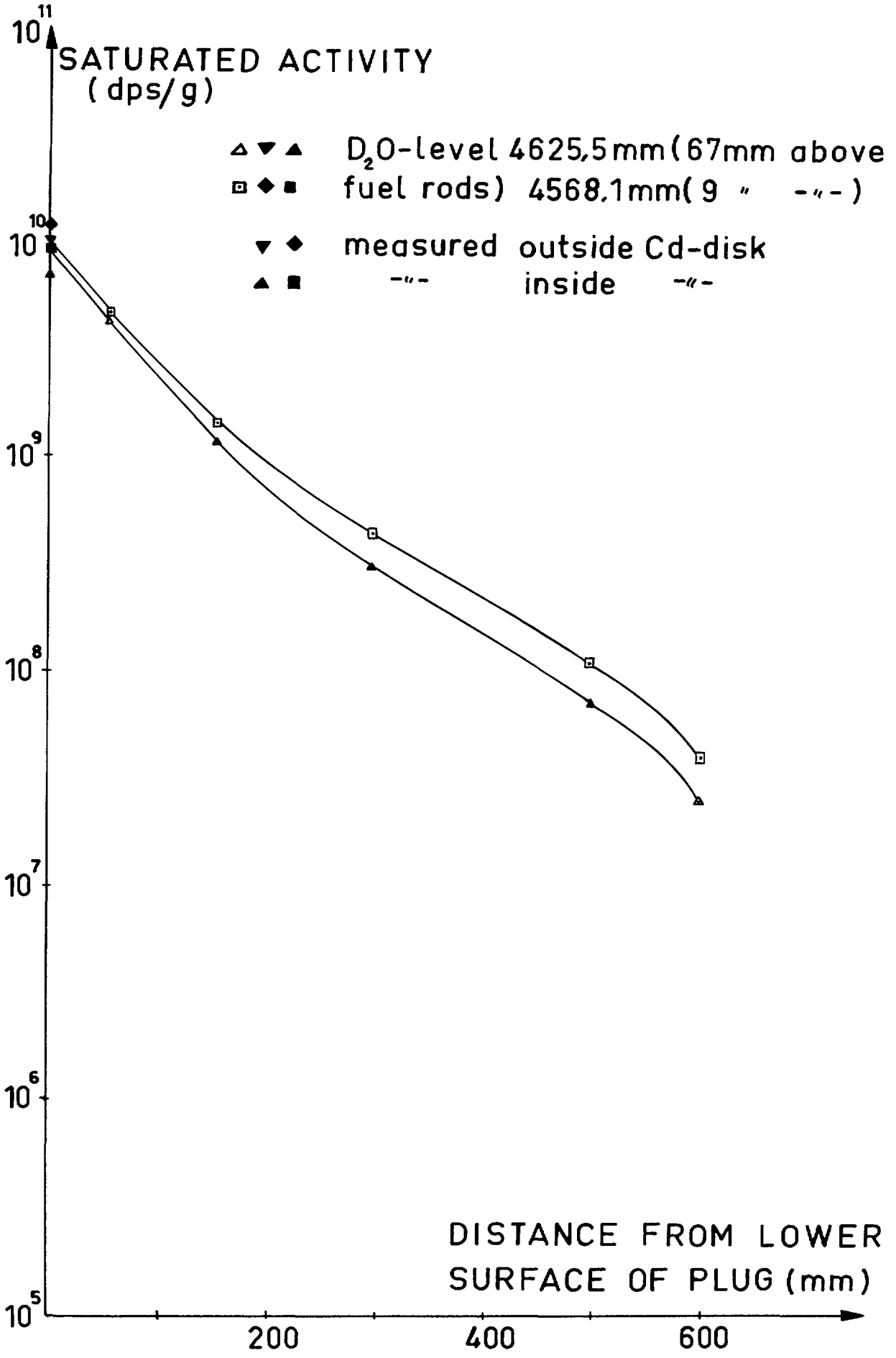

Cu-activity in Iron Plug at Two Different Water-levels (with Cd-disk)
In the interval 0-100 mm the curves have been drawn with the help of figs. 3 and 5.

Fig 4

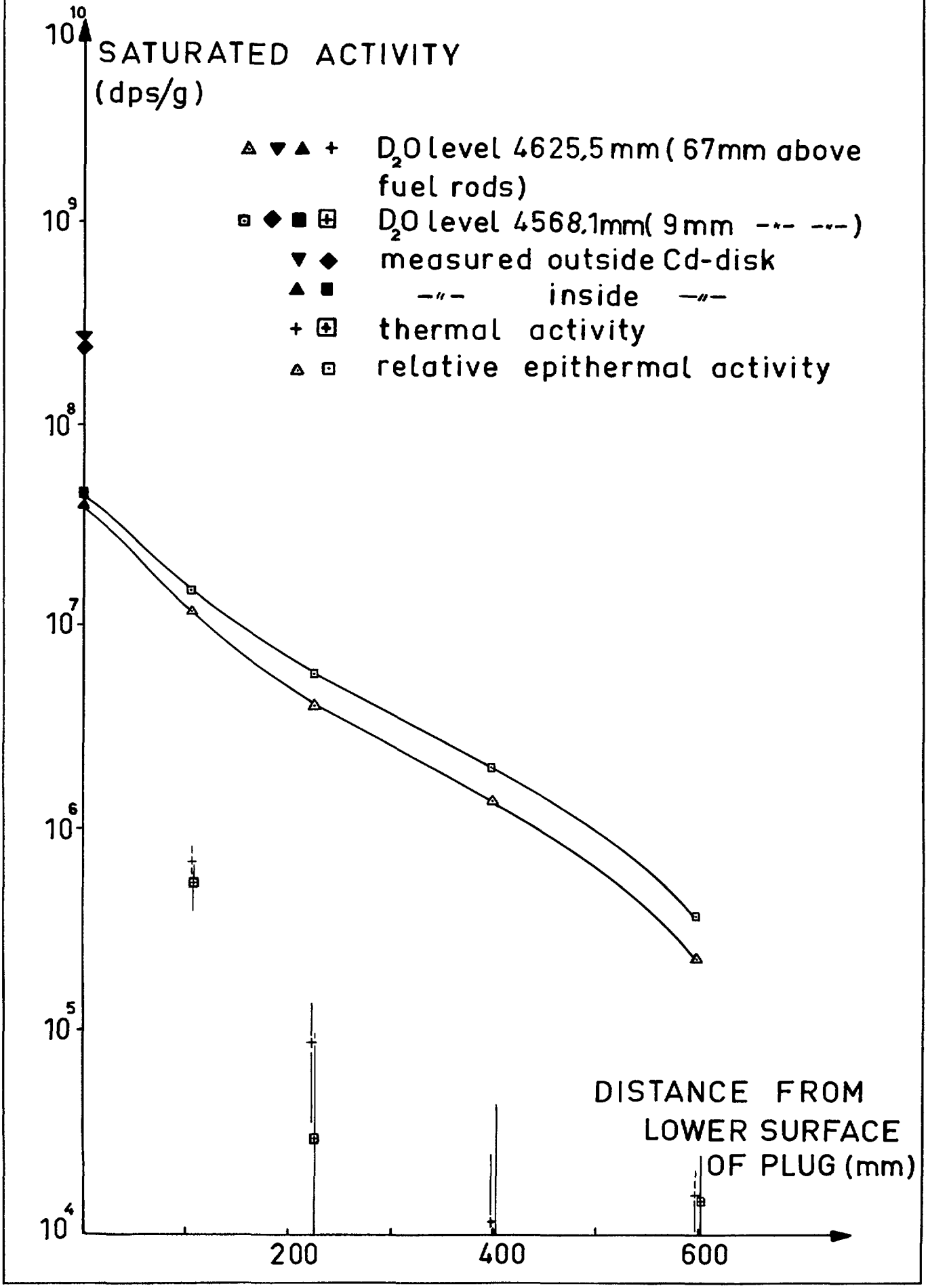

Cu-activity in Lower Part of Iron Plug at Two Different Water-levels(with Cd-disk)

Fig. 5

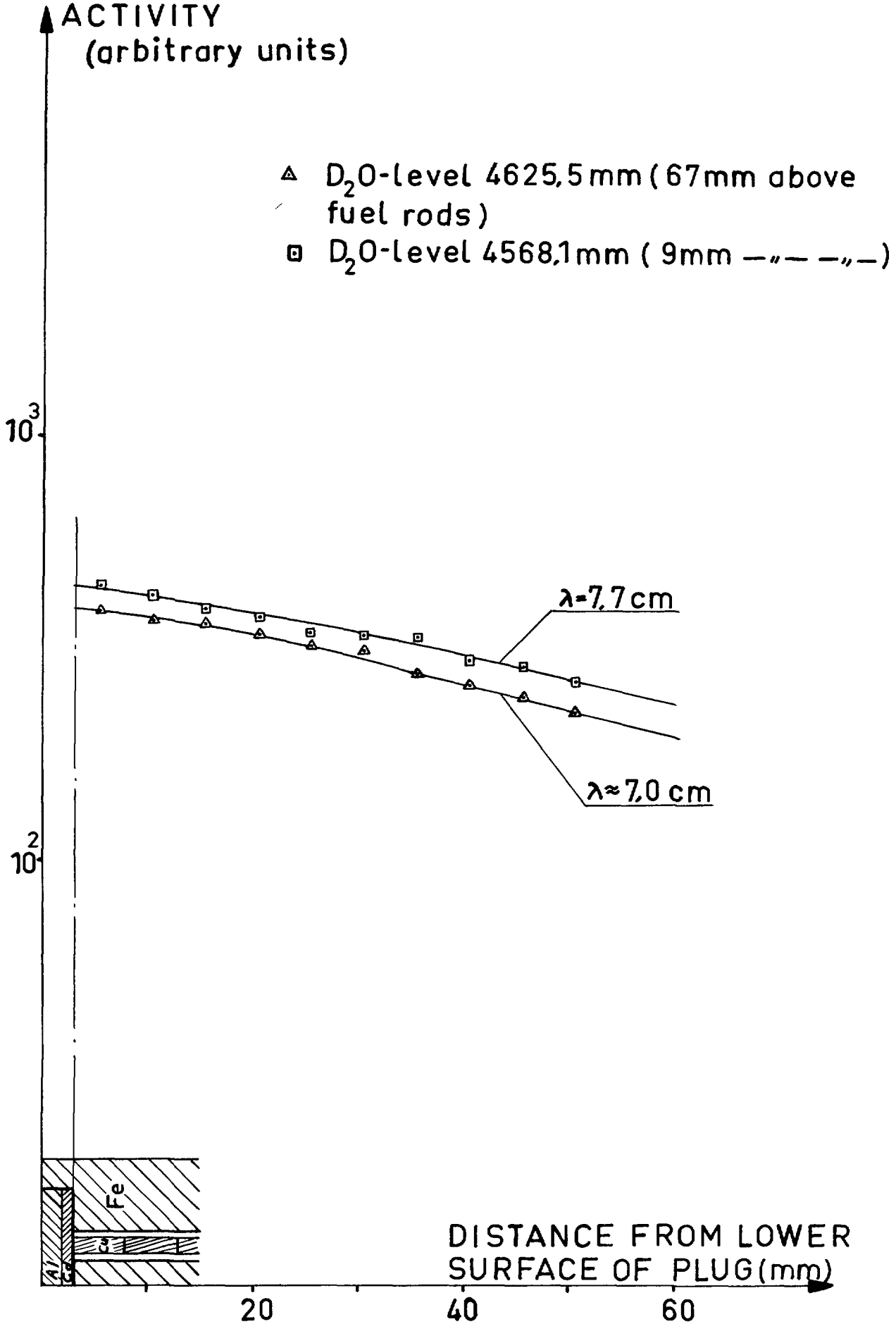

"Fe-activity" in Lower Part of Iron Plug with and without Cd-disk (D_2O-level 4625,5 m.m)

Fig.6

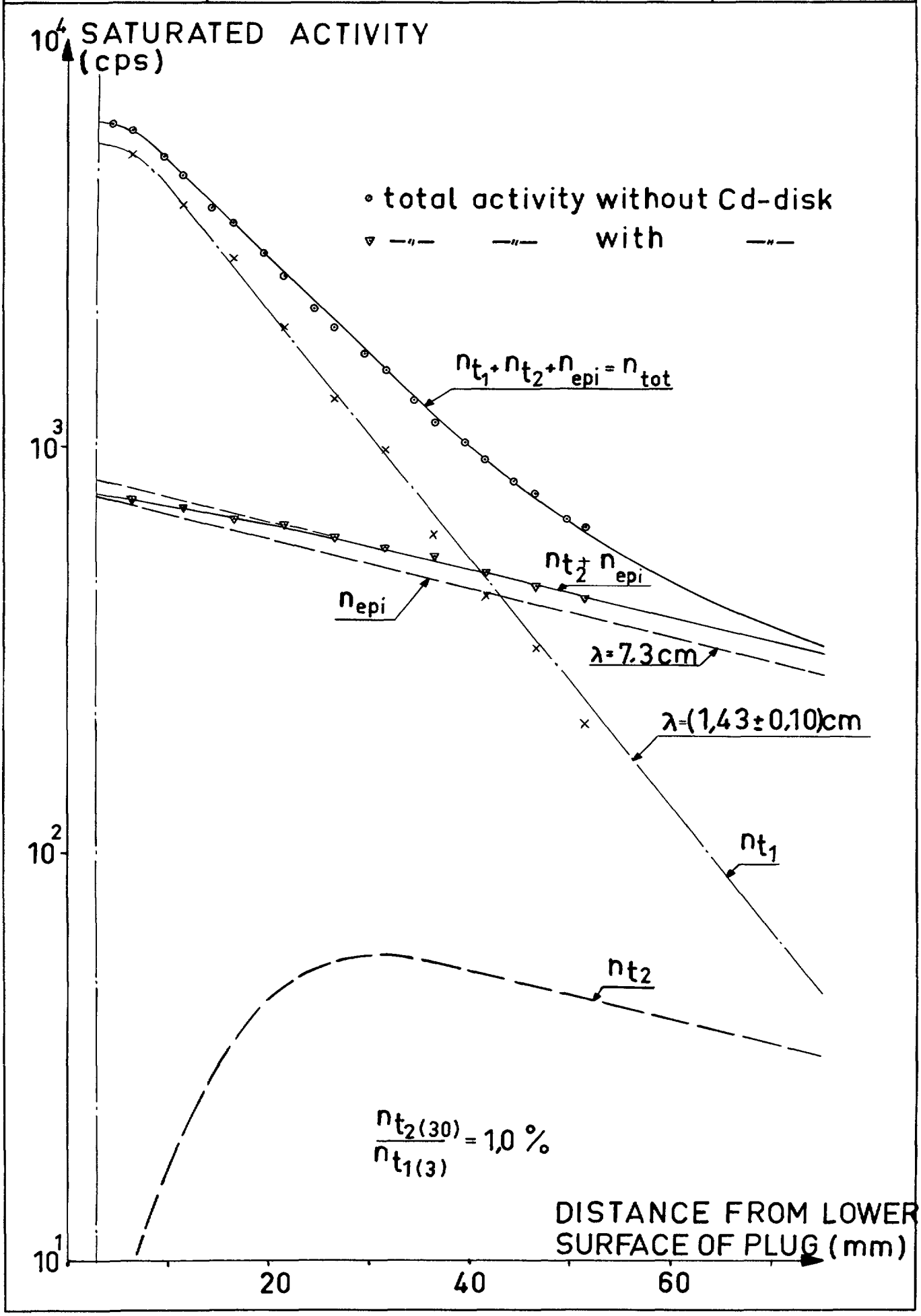

Au-activity in Iron Plug with and without C-d disk
(D_2O level 4625,5mm)

Fig. 7

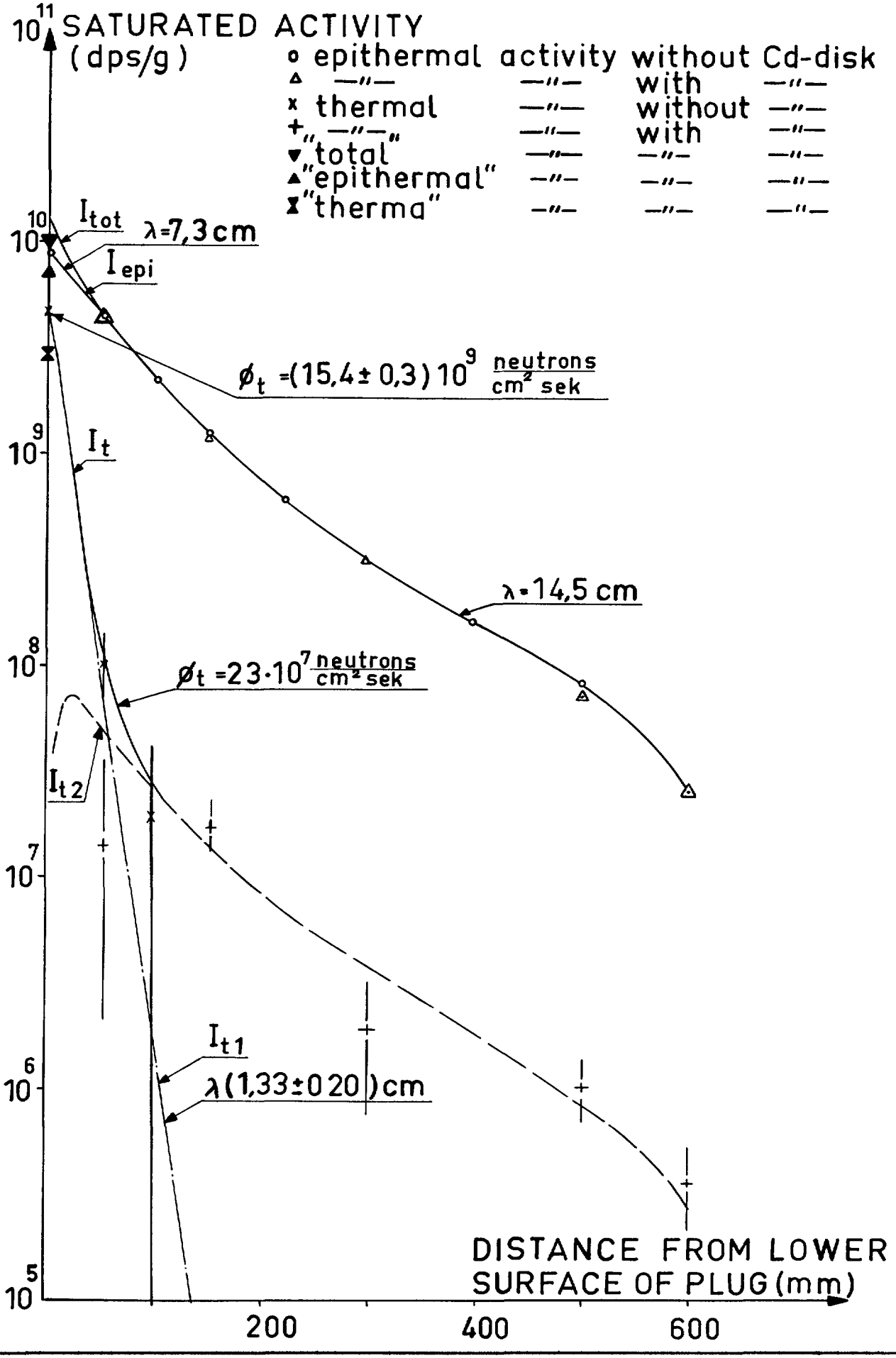

Cu-activity in Iron Plug with and without Cd-disk (D_2O-level 4625,5 mm)

Fig 8

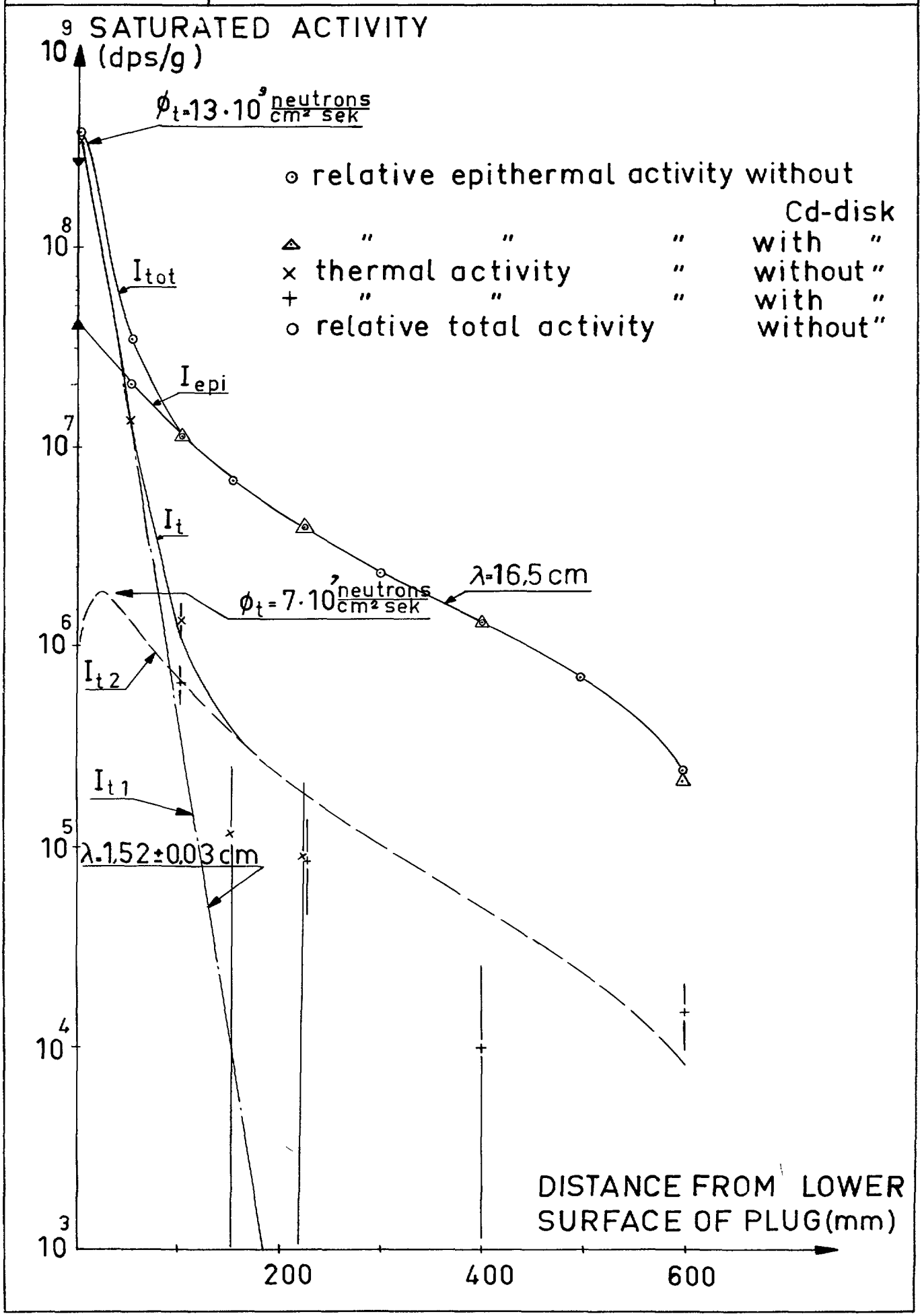

Mn-activity in Iron Plug without Cd-disk (D_2O-level: 4625.5 mm)

Fig. 9

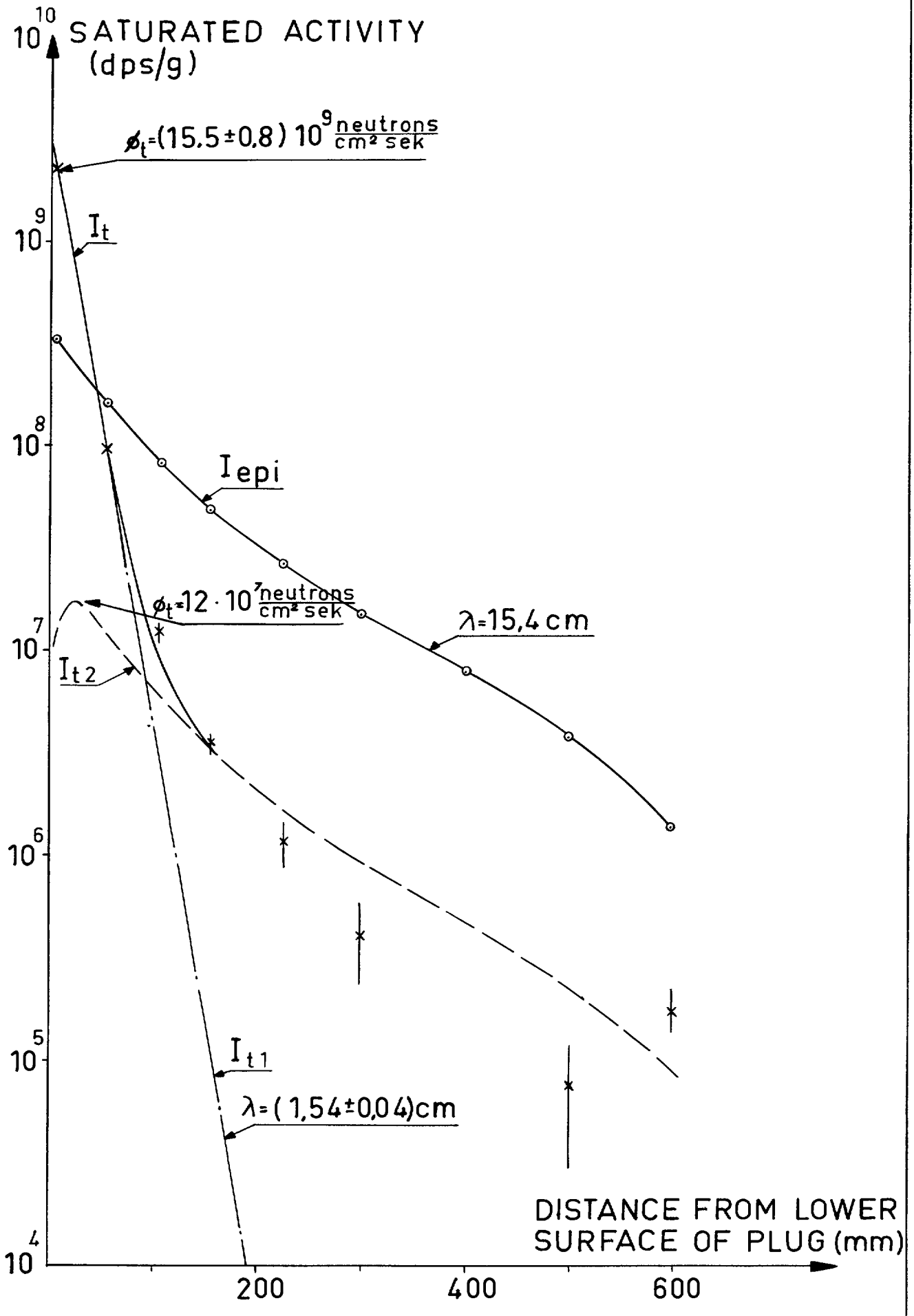

Activity of Cu-ribbon at Bottom of Iron Plug. Cd-disk Removed.

Fig 10

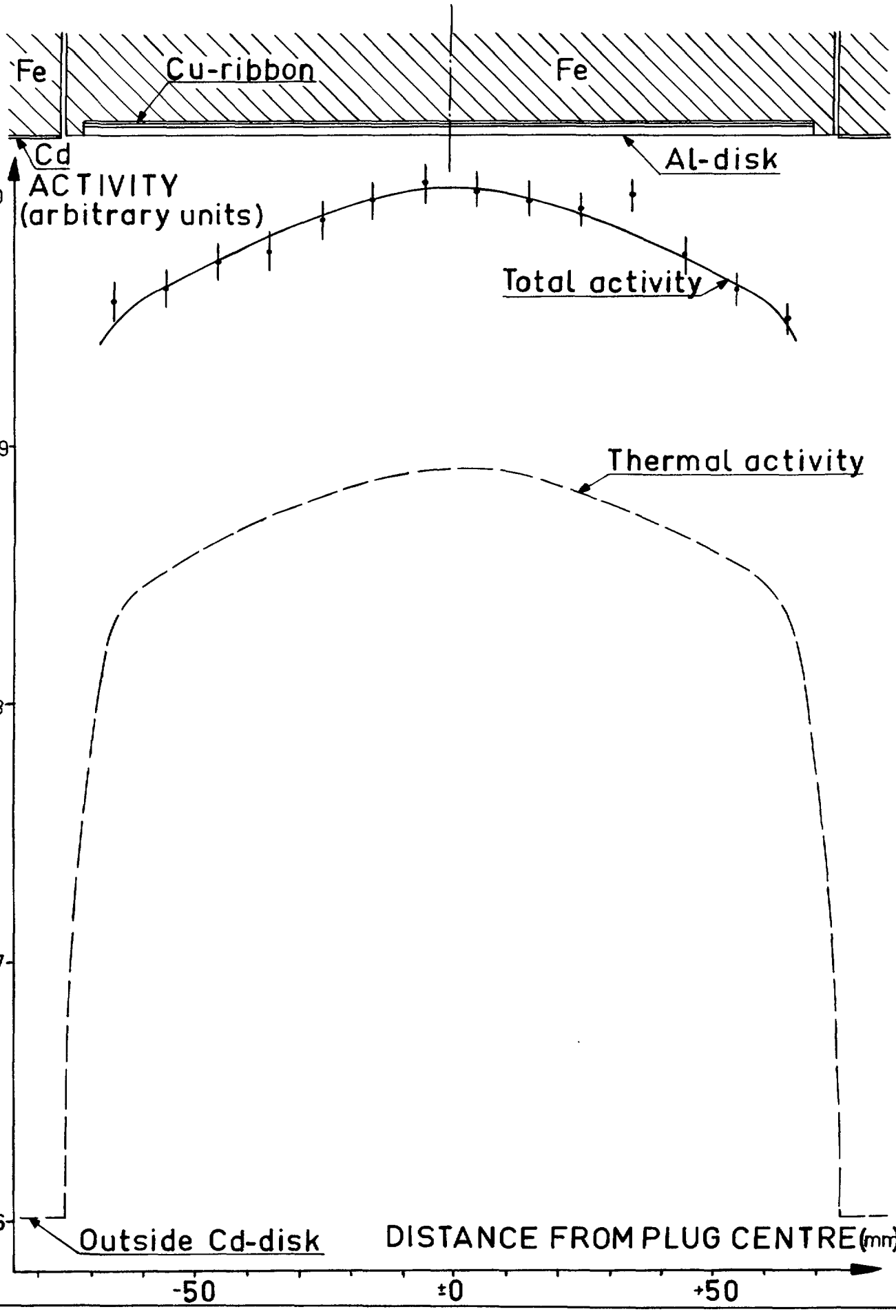

Fig. 11

Fast Flux in Iron Plug Measured with $P^{31}(n,p)S^{31}$ reaction.

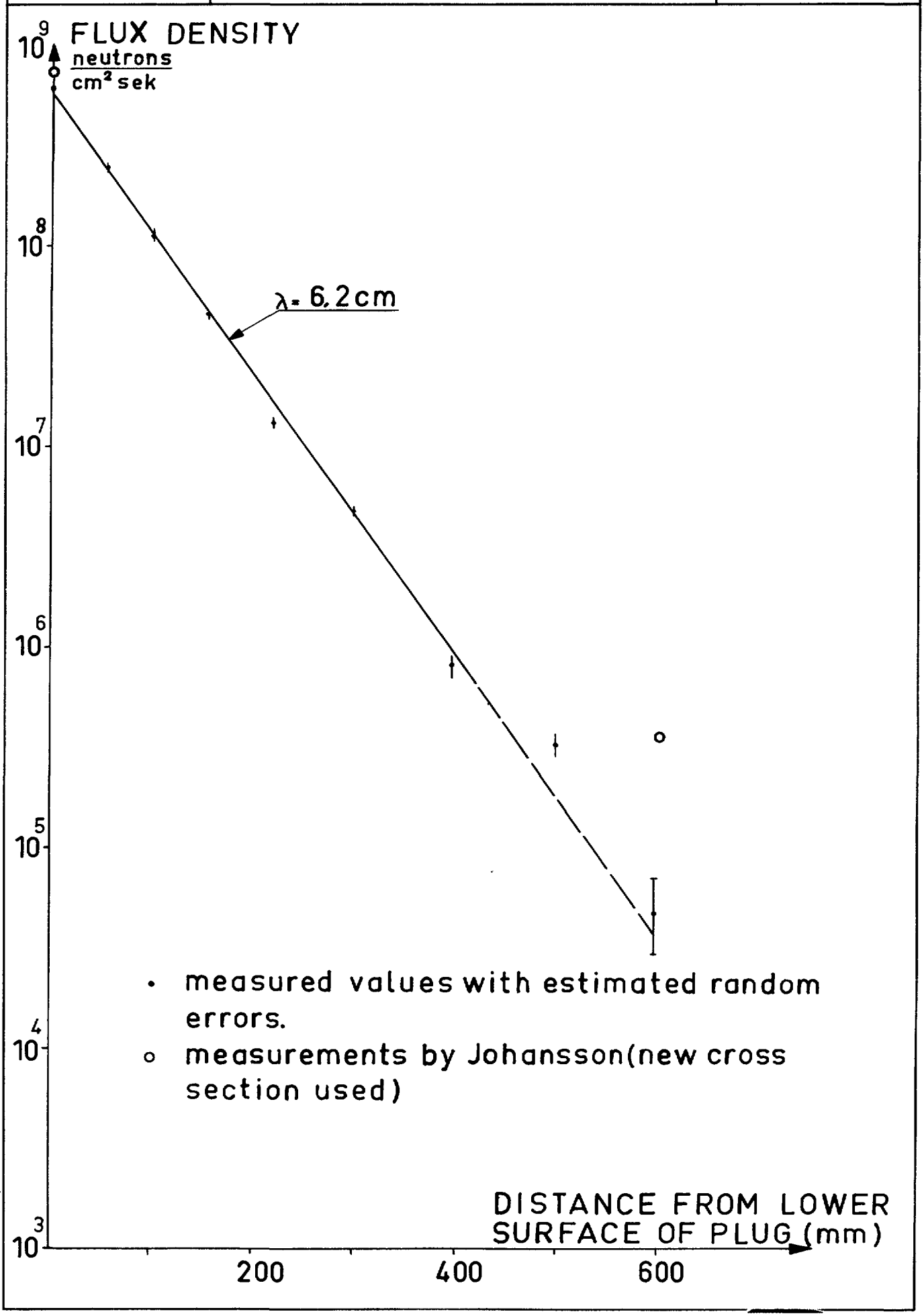

Fig 12

Gamma-ray Dose Rate in Iron Plug without Cd-disk at 1 KW (D_2O-level: 4625,5 mm)

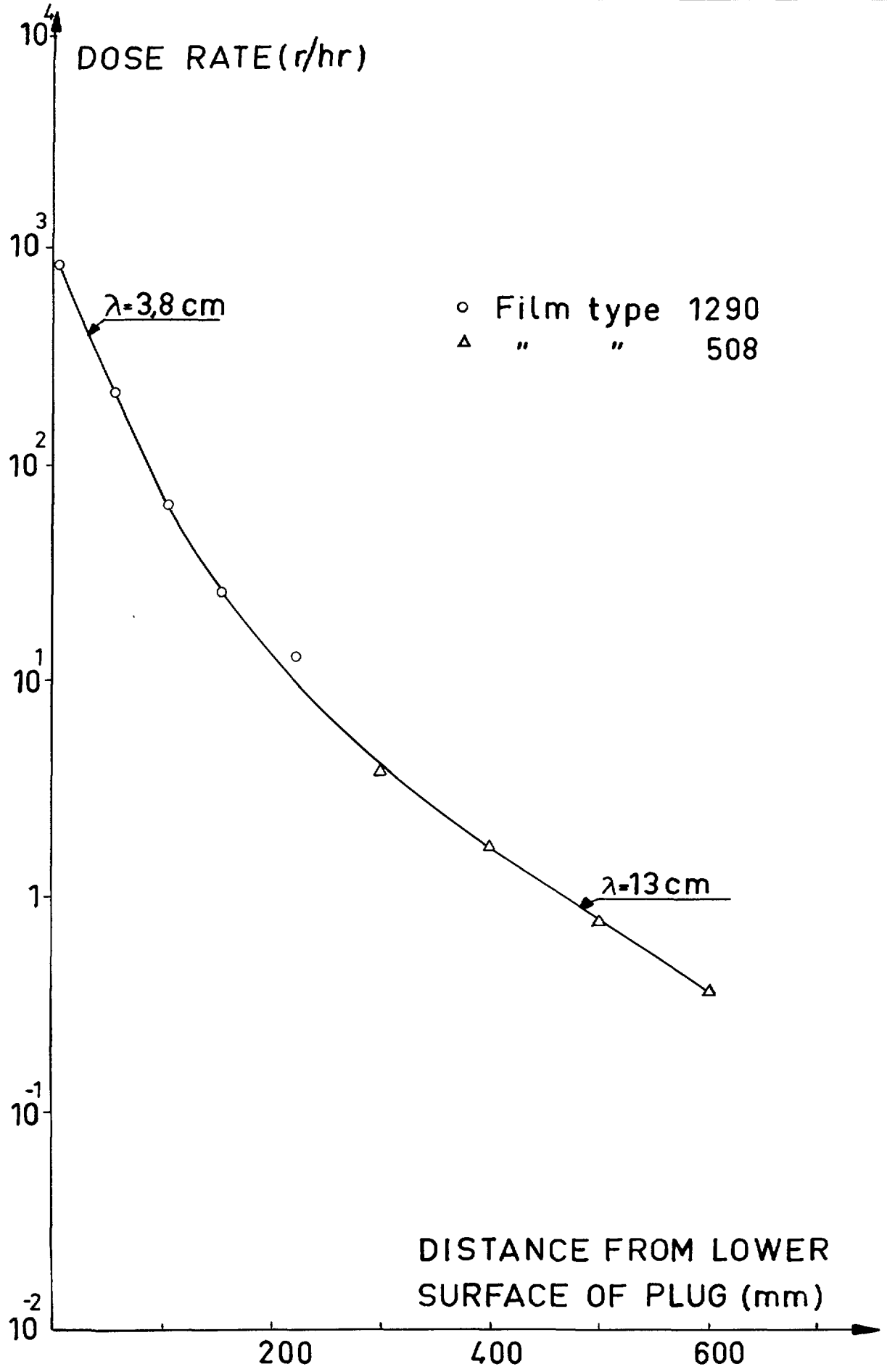

Price Sw. cr. 4:—
Additional copies available at the library of
AB ATOMENERGI
Stockholm - Sweden

Affärstryck Offset 1958.